New substorm index derived from high-resolution geomagnetic field data at low latitude and its comparison with AE and ASY indices

M. Nosé [1], T. Iyemori [1], M. Takeda [1], H. Toh [1], T. Ookawa [2], G. Cifuentes-Nava [3], J. Matzka [4], J. J. Love [5], H. McCreadie [6], M. K. Tunçer [7], and J. J. Curto [8]

[1] Data Analysis Center for Geomagnetism and Space Magnetism, Graduate School of Science, Kyoto University, Japan

[2] Kakioka Magnetic Observatory, Japan Meteorological Agency, Japan

[3] Instituto de Geofisica, Universidad Nacional Autonoma de Mexico, Mexico

[4] Remote Sensing and Geomagnetism, Danish Meteorological Institute, Denmark

[5] United States Geological Survey, United States

[6] Geophysical Observatory, Department of Earth and Environmental Sciences, Ludwig-Maximilians University, Germany

[7] Geomagnetism Laboratory, Kandilli Campus, Boğaziçi University, Turkey

[8] Observatori de L'Ebre, CSIC - Universitat Ramon Llull, Spain

High-resolution geomagnetic field data (i.e., ≤5 seconds) have recently become more commonly used by space physicists. The data permit the identification of Pi2 pulsations, having periods of 40-150 seconds and irregular waveforms. Pulsations of this type appear clearly in time series from mid- and low-latitude ground stations on the nightside at substorm onset. Therefore, with data from multiple observatories, substorm genesis and evolution can be monitored. Here we propose a new substorm index, the Wp index (Wavelet and planetary), which measures Pi2 spectral power at low-latitude. This index is derived from geomagnetic field data obtained from observatories arranged in longitude around the Earth's circumference. Presently, data from 5 ground stations (Fürstenfeldbruck, Iznik, Urumqi, Kakioka, and Teoloyucan) are used, but future work will include data from other sites as well (Honolulu, Tucson, San Juan, Tristan da Cunha, and Ebro). Here we compare substorm occurrence estimated from the Wp index and those from the AE and ASY indices. We show that Wp index is a good indicator of substorm onset.

1. Introduction

Substorms are one of the most distinguished phenomena in the geospace. Their occurrence can be identified in a number of different ways, including auroral breakup, energetic particle injection in the inner magnetosphere, magnetic field dipolarization, magnetic reconnection in the magnetotail, and plasmoid development in the distant tail. In terms of ground-base geomagnetic field data, substorms can be identified by high-latitude negative bays and mid-latitude positive bays. There are geomagnetic indices which reflect occurrence of high-latitude negative bays and mid-latitude positive bays; the AE index is for the former [*Davis and Sugiura*, 1966] and the ASY index is for the latter [*Iyemori and Rao*, 1996]. These indices are derived from multiple stations distributed in longitude around the globe. Data from 12 stations and 6 stations contribute to the AE index and the ASY index, respectively.

Pi2 pulsations are defined as geomagnetic variations with periods of 40-150 seconds and irregular (damped) waveforms [*Jacobs et al.*, 1964]. Previous studies reported that Pi2 pulsations can serve as an diagnostic indicator of substorm onset. They appear almost simultaneously with auroral breakups [e.g., *Gelpi et al.*, 1987], energetic particle injection in the inner magnetosphere [e.g., *Saka et al.*, 1996], and magnetic field dipolarization [e.g., *Yumoto et al.*, 1989]. Since low-latitude Pi2 pulsations have dominant power near the midnight, multiple ground stations distributing longitudinally are needed for their detection. Recently a large number of geomagnetic observatories have started recording geomagnetic field variations with 1-sec time resolution. This development facilitates the routine derivation of a new index measuring Pi2 power. In this study, using data from the longitudinal network of 5 ground stations, we propose a new substorm index, the "Wp index" (Wavelet and planetary).

2. Longitudinal Network of Ground Stations

Figure 1 shows the locations of geomagnetic stations used to derive the Wp index. The coordinates of the stations are listed in Table 1. Filled red circles in Figure 1 represent geomagnetic stations which are now under operation in acquisition of high time resolution of geomagnetic field data. Their names (3-letter abbreviation code, sponsoring country) are Fürstenfeldbruck (FUR, Germany), Iznik (IZN, Turkey), Urumqi (UMQ, China), Kakioka (KAK, Japan), and Teoloyucan (TEO, Mexico). Time resolution of data is 1 second, except for Teoloyucan which provides 5-second resolution data. The largest longitudinal separation between stations is about 120° (between TEO and KAK/FUR), thus at least one station is always positioned on the nightside where low-latitude Pi2 pulsations can be clearly observed. In the following study, we processed data from these 5 stations by wavelet analysis and derived the Wp index. Stations which might be included in the future are also summarized in Table 1 and shown with open red circles in Figure 1.

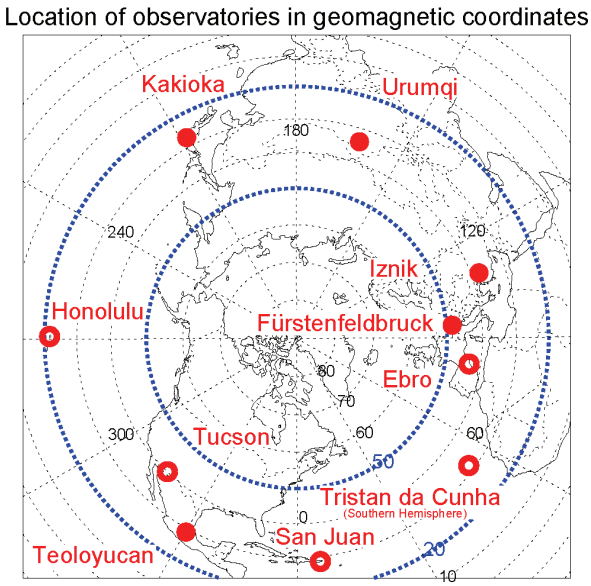

Figure 1. Location of geomagnetic stations in geomagnetic coordinates used to derive the Wp index. Dotted blue circles indicate geomagnetic latitudes of 20° and 50°. Filled red circles represent stations measuring geomagnetic field variations with a high time resolution. Open red circles show stations from which high time resolution data will become soon available.

3. Method of Calculation of Wp Index

3.1. Wavelet analysis

Wavelet analysis is similar to Fourier analysis in that a time series is decomposed into orthonormal basis functions. Here we briefly summarize wavelet analysis that is described by *Nosé et al.* [1998] in more detail. In Fourier analysis, harmonic functions ($e^{i2\pi ft}$, where f is frequency and t is time) are adopted as orthonormal basis functions. Let *h(t)* and *H(f)* be a given function in the time domain and its Fourier transform in the frequency domain. The Fourier transform equations can be expressed by

$$h(t) = \int_{-\infty}^{\infty} H(f) \cdot e^{i2\pi ft} df,$$

$$H(f) = \int_{-\infty}^{\infty} h(t) \cdot (e^{i2\pi ft})^* dt,$$

where the asterisk denotes the complex conjugate. The Fourier transform is very popular in analysis of time series data, in particular, periodic signals; but it has a limitation which comes from the characteristics of the harmonic functions. Since the harmonic functions have finite values for $t \rightarrow \pm\infty$, Fourier analysis is sometimes not appropriate to analyze phenomena localized in time.

In wavelet analysis, a time series is decomposed into the orthonormal basis functions which are localized in time and limited in a specific frequency range (wavelets). Thus wavelet analysis is a suitable method for investigating the wave power of phenomena which are limited in both time and frequency, such as Pi 2 pulsations. The time series is mapped to the time-frequency domain, so the wavelet transform has two parameters which correspond to time and frequency. For a time series *x(t)*, the wavelet transform is expressed as

$$x(t) = \sum_j \sum_k \alpha_{j,k} \cdot \psi_{j,k}(t),$$

$$\alpha_{j,k} = \int_{-\infty}^{\infty} x(t) \cdot \psi^*_{j,k}(t)\, dt,$$

where $\alpha_{i,k}$ is the wavelet coefficient and $\psi_{i,k}$ is the discrete wavelet set. $\psi_{i,k}$ is constructed from an analyzing wavelet $\phi(t)$, which generates the orthonormal wavelet set, by

$$\psi_{j,k}(t) = \phi\left(2^j t - k\right),$$

where j and k are integers. This equation indicates that j is related to the dilation or contraction of $\phi(t)$ and k is related to the shift of $\phi(t)$ in the time domain. Thus j and k can be considered as parameters of frequency (dilation) and time (translation), respectively. A number of analyzing wavelets to generate the orthonormal wavelet set have been found. For example, the Haar wavelet, the

(degree)

Station	Code	GGLAT	GGLON	GMLAT[1]	GMLON[1]	Status
San Juan	SJG	18.11	293.85	28.31	6.08	Planned
Tristan da Cunha	TDC	-37.25	347.50	-31.55	53.42	Planned
Ebro	EBR	40.82	0.50	43.18	81.31	Planned
Fürstenfeldbruck	FUR	48.17	11.28	48.39	94.58	Operating
Iznik	IZN	40.50	29.73	37.74	109.58	Operating
Urumqi	WMQ	43.80	87.70	34.11	162.21	Operating
Kakioka	KAK	36.23	140.19	27.37	208.71	Operating
Honolulu	HON	21.32	202.00	21.64	269.74	Planned
Tucson	TUC	32.17	249.27	39.88	316.11	Planned
Teoloyucan	TEO	19.75	260.82	28.76	330.34	Operating

[1] Values in January 2005

Table 1. Coordinates of ground stations used in derivation of the Wp index. GGLAT and GGLON denote geographic latitude and longitude. GMLAT and GMLON mean geomagnetic latitude and longitude.

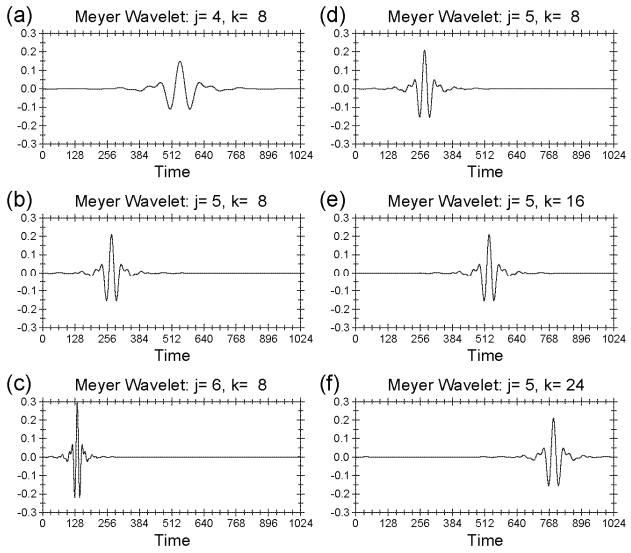

Figure 2. Wavelet functions $_{j,k}(t)$ which are generated from the Meyer wavelet with =1024 and (j, k) of (a) (4,8), (b) (5,8), (c) (6,8), (d) (5,8), (e) (5,16), and (f) (5,24).

Daubechies wavelet [*Daubechies*, 1988], and the Meyer wavelet [*Meyer*, 1989] are known. In this study we used the Meyer wavelet, because the Meyer wavelet is band-limited in frequency [e.g., *Sasaki et al.*, 1992; S*ato and Yamada*, 1994; Y*amada and Ohkitani*, 1991; *Yamanaka et al.*, 1994; *Yomogida*, 1994] as same as Pi2 pulsations (i.e., 6.67-25.0 mHz).

For actual analysis we use a discrete time series and take a finite data segment. Assuming a time series which has a sampling rate and a number of data points N ($N = 2^n$, n is integer), we will obtain wavelet coefficients $\alpha_{i,k}$ confined in $0 \le j \le n-1$ and $0 \le k \le 2^j-1$. The frequency band for each j is $2^j/3T \le f \le 2^{j+2}/3T$, where is the data length $T = Ndt$). Note that the widths of time window and frequency window covered by $\alpha_{i,k}$ are $T/2^j$ and $2^j/T$, respectively. This indicates that the wavelet coefficient with a large value of j has high resolution in time and low resolution in frequency, and vice versa. The Nyquist frequency is included in the frequency range supported by the maximum value of j.

Figure 2 shows waveforms of the wavelet functions $\psi_{i,k}$ which are generated from the Meyer wavelet with N=1024=2^{10}. Note that the Meyer wavelet has a symmetric waveform. From Figures 2a-2c which give examples of wavelet functions with different values of (i.e., j=4-6), we see that the wavelet function with a smaller value of is more dilated than that with a larger value of j. Figures 2d-2f display examples of wavelet functions with different values of k (i.e., j=8, 16, 24). For a smaller value of k, the non-zero part of the wavelet function appears earlier in time. Therefore we can discuss phenomena from the viewpoint of both frequency (j) and time (k) at once. Even if more than one wave packets having an identical frequency appear at different times, these phenomena are identified by wavelet coefficients with different values of k.

3.2. Calculation Procedure

Using the 1-second data from the 5 stations, we calculate the Wp index as follows. (Since TEO data have a time resolution of 5 seconds, interpolation was performed to create 1-second data.) Schematic figure of calculation procedure is shown in Figure 3.

1. Wavelet analysis is applied to geomagnetic field data for a segment of 512 second length. The data segment is shifted forwards by 60 seconds and the wavelet analysis is repeated (Figure 3a). This process is conducted for both the H and D components from individual stations.

2. Using the obtained wavelet coefficients, we calculate wavelet power with time resolution of 1 minute (Figure 3b). The frequency bands of wavelet function with j=4 and 5 are 5.2-20.8 mHz and 10.4-41.7 mHz, respectively, which cover a frequency range of Pi2 pulsations (6.67-25.0 mHz). Thus the wavelet power ( ) is defined as an average of wavelet coefficients of j=4 and 5 ($\alpha_{4,k}$ and $\alpha_{5,k}$) in a given 1-minute bin. This process results in a time series of 1-minute wavelet power (i.e., 1440 data points/1 day) for each component and each station. (Careful readers may notice that the frequency bands of wavelet function are derived in the case of N=1024. This is because we added 256 data points artificially to both ends of the 512-second data segment before wavelet analysis; the additional data are given to be equal to each end of the data segment. If the time series is tapered by the data window function as done in the Fourier analysis, the results become inappropriate around each end.)

3. Since amplitude of Pi2 pulsations is dependent on geomagnetic latitude [e.g., *Osaki et al.*, 1996], the wavelet

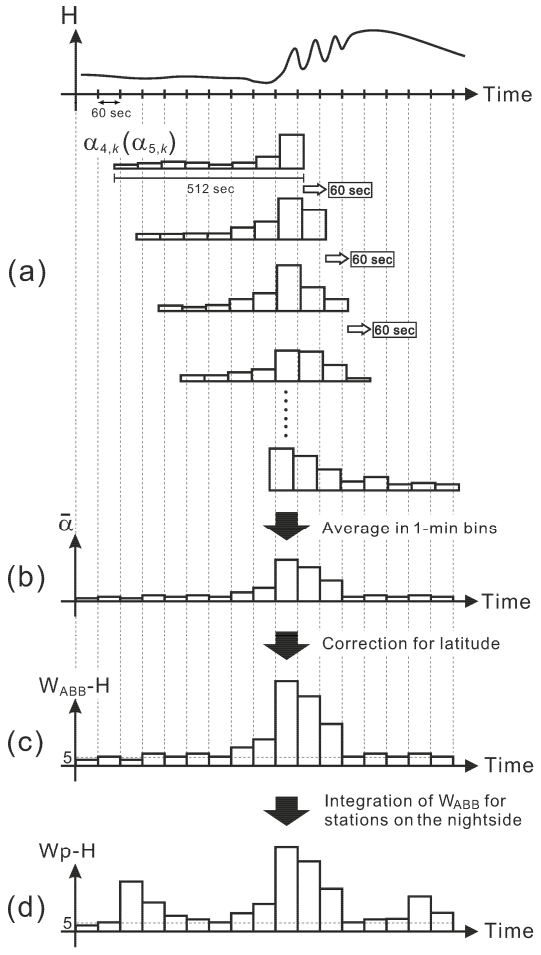

Figure 3. Schematic figure of calculation procedure of the Wp index.

power should be corrected for that (Figure 3c). First we compute a baseline of the wavelet power ($P_{Baseline}$) on monthly basis. The baseline is derived by averaging the 1-minute wavelet power for 1800-0600 magnetic local time (MLT) of the 5 international quietest days, that is, 3600 data points. Then 1-minute wavelet power is multiplied by $5/P_{Baseline}$ and rounded to the nearest integer, yielding time series of the corrected wavelet power in which the baseline becomes a constant value of 5 for all components and all stations. The corrected wavelet power is expressed as W_{ABB}-C, where ABB is the 3-letter IAGA code for geomagnetic observatories and C is the component. For example, W_{KAK}-H stands for the corrected wavelet power for the H component at Kakioka.

4. The Wp index (Wp-H and Wp-D) is derived from W_{ABB} (W_{ABB}-H and W_{ABB}-D). Since Pi2 pulsations have dominant power on the nightside, we use only W_{ABB} from stations located at 1800-0600 MLT. The Wp index is simply defined as an average of W_{ABB} of the stations on the nightside (Figure 3d).

3.3. Example of Calculation for September 28, 2005

Following the procedure described in the previous subsection, we calculated the Wp index for September 28, 2005, using data of the 5 available stations. Top 5 panels of Figure 4 display the corrected wavelet power in the H component (W_{ABB}-H) derived with Procedures 1-3 for each station. A horizontal green bar in each panel indicates local nighttime (1800-0600 MLT) of the station. During 0100-0200 UT, IZN and FUR are on the nightside and enhancements of W_{IZN}-H and W_{FUR}-H are seen. Around 0500 UT and 0615 UT, TEO was on the nightside and showed enhancements of W_{TEO}-H, which are also seen at KAK though it was in the afternoon sector. Around 1400 UT, both KAK and WMQ were located on the nightside and observed increases of W_{KAK}-H and W_{WMQ}-H. From 1700 UT to 1715 UT, 4 of 5 stations (KAK, WMQ, IZN, and FUR) found large increases of the corrected wavelet power at nighttime. All of these enhancements are expected be occurrence of Pi2 pulsations, because they are found at local nighttime.

From time series of the corrected wavelet power, we calculate the Wp-H index with Procedure 4. Bottom panel of Figure 4 shows the result of calculation, that is, the Wp-H index. We can see significant increases of the Wp-H index as indicated by vertical arrows around 0045 UT, 0130 UT, 0145 UT, 0500 UT, 0615 UT, 1330 UT, 1400 UT, 1700 UT, and 1715 UT, which were already identified in the corrected wavelet power (top 5 panels of Figure 4). Therefore the Wp index can be thought as "a global index", which reflects nighttime wave power in the Pi2 frequency range at any given UT time.

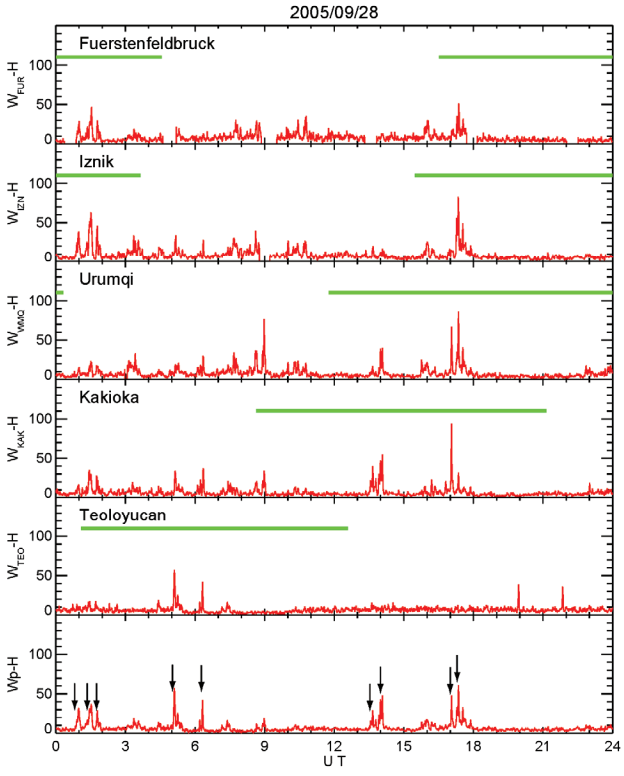

Figure 4. (1st to 5th panels) Corrected wavelet power in the H component, W_{ABB}-H, for 5 available stations for September 28, 2005. From top to bottom, W_{FUR}-H, W_{IZN}-H, W_{WMQ}-H, W_{KAK}-H, and W_{TEO}-H are shown. A horizontal green bar in each panel means local nighttime (1800-0600 magnetic local time) of the station. (6th panel) Wp-H index for September 28, 2005 calculated from W_{ABB}-H shown in the 1st to 5th panels. Vertical arrows indicate times of clear enhancements in the Wp index.

4. Comparison of Wp Index with Other Substorm Indices

4.1. Case study

Now we compare substorm signatures found in the Wp index and those found in the AE index and the ASY index. Enhancement of the Wp index is considered as occurrence of Pi2 pulsations at low-latitude, while increases of the AE and ASY indices are interpreted as occurrence of

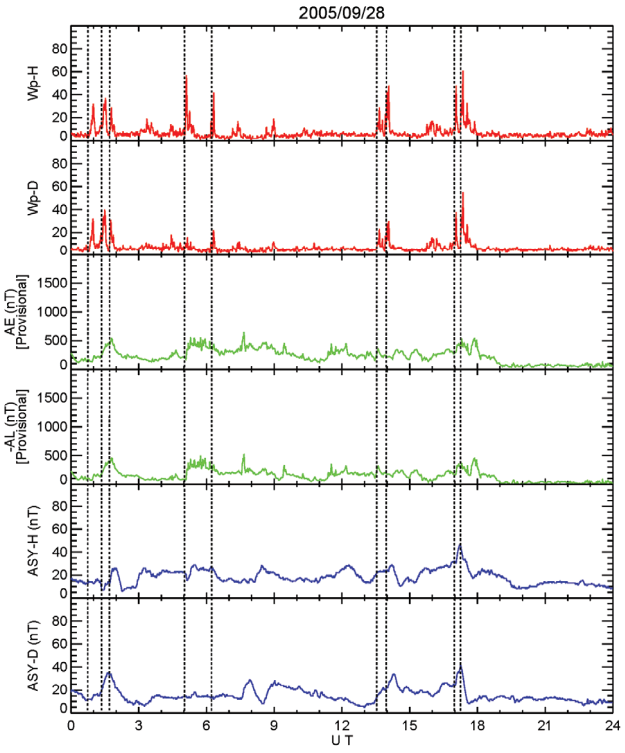

Figure 5. Stack plots of the Wp-H, Wp-D, AE, AL (-AL), ASY-H, ASY-D indices for September 28, 2005. For intercomparison among these indices, vertical dotted lines are drawn at times of the Wp enhancements, which are the same time as vertical arrows in Figure 4.

	Wp	AE	AL	ASY-H	ASY-D	LANL
Substorm Signature	Low-latitude Pi2	High-latitude Negative Bay		Mid-latitude Positive Bay		Particle Injection
0045 UT	Yes	No	No	No	No	Yes
0130 UT	Yes	Yes	Yes	Yes	Yes	Yes
0145 UT	Yes	No	No	No	No	Yes
0500 UT	Yes	Yes	Yes	Yes	No	Yes
0615 UT	Yes	No	No	No	No	Yes
1330 UT	Yes	No	No	Yes	Yes	Yes
1400 UT	Yes	No	No	No	No	Yes
1700 UT	Yes	Yes	Yes	Yes	Yes	Yes*
1715 UT	Yes	No	No	No	No	Yes*

Table 2. Summary of comparison between the Wp index and other substorm indices/satellite data for September 28, 2005. Detail description is found in Section 4.1. "Yes*" means that the particle injection corresponds to either of the two Wp enhancements.

high-latitude negative bay and mid-latitude positive bay. Top panel of Figure 5 is the Wp-H index which is identical to the bottom panel of Figure 4. The Wp-D index is also calculated in the same way as the Wp-H index and displayed in the second panel of Figure 5. Both indices are similar to each other, except for values around 0500 UT. For comparison among geomagnetic indices, plots of the AE, AL (-AL), ASY-H, and ASY-D indices for September 28, 2005 are also given in the third to sixth panels of Figure 5.

For the Wp increase at 0130 UT, the AE, -AL, ASY-H, and ASY-D indices were also increased. However, no corresponding changes can be found in the AE, -AL, and ASY indices for 0045 UT and 0145 UT. A significant increase was found in the Wp-H index at 0500 UT, and this is accompanied by increases of the AE, -AL, and ASY-H indices. At 0615 UT, clear substorm signatures appeared only in the Wp index. There are enhancements in the Wp and ASY indices for 1330 UT, while clear increases are found only in the Wp index at 1400 UT. At 1700 UT all of indices showed enhancements, confirming substorm occurrence, though at 1715 UT no enhancement appeared in the AE, -AL, and ASY indices. Substorm occurrence can be also identified with energetic particle injections at geosynchronous altitude, thus the Wp index is compared with data from LANL geosynchronous satellite. Only a single satellite (1990-095) was available for September 28, 2005. Data plot is not shown here, but can be browsed from http://leadbelly.lanl.gov/lanl_ep_data. For the first 7 increases of Wp (0045 UT, 0130 UT, 0145 UT, 0500 UT, 0615 UT, 1330 UT, and 1400 UT), energetic electron flux showed clear enhancements. There was an electron flux increase around 1700 UT, but it is not clear which of the 1700 UT or 1715 UT enhancements of the Wp index is associated with the flux enhancement. This is because the 1990-095 satellite was on the dayside and the flux increase showed energy dispersion.

Table 2 summarizes the comparison of the Wp index with other substorm signatures. Three of 9 Wp index increases (at 0130 UT, 0500UT, and 1700 UT) are associated with substorm signatures of the AE, AL, and ASY indices. This may be caused by insensitivity of the AE, AL, and ASY indices to small substorm onsets or pseudo-substorm onsets, while the Wp index, that is, low-latitude Pi2 pulsation, is sensitive to such substorm onsets [e.g., *Sakurai and Saito*, 1976]. Moreover, a number of stations used to derive the AE and AL indices are 9-10 for 0000-2100 UT on September 28, 2005 with lack of stations in Russian territory, suggesting that substorms cannot be detected with the AE and AL indices when Russian stations are near midnight (approximately 1300-2100 UT) [e.g., *Takahashi et al.*, 2004]. Thus we think that the Wp index is still a useful index to detect substorm onset, and this idea is supported by a fact that 8 substorm onsets identified by the Wp index are accompanied by energetic electron flux enhancements at geosynchronous orbit.

4.2. Statistical study

We performed a correlation analysis between the Wp-H index and other substorm indices. Results for 1 month interval of September 2005 are shown in Figure 6. Each of 4 panels shows relation between the Wp-H index and the AE/-AL/ASY-H/ ASY-D index. Small dots represent 1-min data points and large circles are average values in 10-nT bins of the Wp-H index. Correlation coefficients

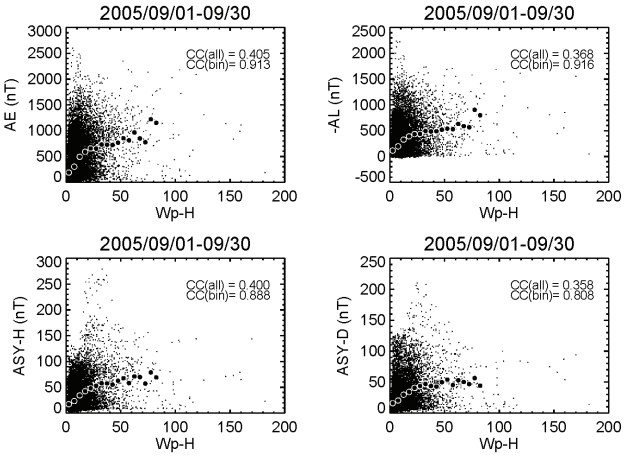

Figure 6. Relation between the Wp-H index and the AE/-AL/ASY-H/ASY-D index for September 2005. Small dots are 1-min data points and large circles are average values in 10-nT bins of the Wp-H index. Correlation coefficients for both the all data points (small dots) and the binned-average values (large circles) are shown in upper right corner of each panel.

were computed for both the all data points (small dots) and the binned-average values (large circles), and the results were indicated in upper right corner of each panel of Figure 6. For all data points correlation coefficients are 0.36-0.40, while for binned-average data they are as high as 0.80-0.92. This suggests that the Wp index is suitable to monitor substorm occurrence in addition to the AE and ASY indices.

5. Database of Wp index

Stack plots of the Wp, AE, and ASY indices in the same format as Figure 5 can be obtained from http://s-cubed.info. Such plots are useful for users to identify substorm onset from three different kinds of view points, that is, low-latitude Pi2 pulsation, high-latitude negative bay, and mid-latitude positive bay.

6. Summary

Using geomagnetic field data with high time resolution from 5 low-latitude stations (i.e., Fürstenfeldbruck, Iznik, Urumqi, Kakioka, and Teoloyucan), we proposed a new substorm index, the Wp index, which is related to wave power of low-latitude Pi2 pulsations. In derivation of the Wp index, we adopted wavelet analysis which is a suitable method for investigating the power of short-lived waves, such as Pi 2 pulsations. The above 5 stations are distributed over the globe in longitudinal direction with maximum separation between neighboring stations of ~120°. Thus at least one station is located on the nightside where Pi2 pulsations have dominant power. Since we used only geomagnetic stations on the nightside, the Wp index can be considered as "a global index", which means an index reflecting Pi2 wave power during local nighttime at any given UT time.

We made a comparison of substorm occurrence estimated from the Wp index and those from the AE and ASY indices, in terms of a case study and a statistical study. The Wp index appeared to be a good indicator for substorm onset along with the AE and ASY indices.

Plots of the Wp index are available from the WWW page (http://s-cubed.info). The plots are supplied with the AE and ASY indices, thus it would be easier for users to identify substorm occurrence. In future we will also use high time resolution data from Honolulu, Tucson, San Juan, Tristan da Cunha, and Ebro. This will increase a number of stations in the longitudinal network to be 10, and result in improvement of the Wp index.

Acknowledgments. This work was supported by The Kurata Memorial Hitachi Science and Technology Foundation (grant 844), The Japan Securities Scholarship Foundation (grant 1368), Inamori Foundation, and The Minitstry of Education, Science, Sports, and Culture, Grant-in-Aid for Young Scientists (B) (grant 19740303). Kakioka Magnetic Observatory, China Earthquake Administration, Universidad Nacional Autonoma de Mexico, Danish Meteorological Institute, United States Geological Survey, Ludwig-Maximilians University, Boğaziçi University, and Observatori de L'ebre are acknowledged for their continued support of the observatories.

References

Daubechies, I., Orthonormal bases of compactly supported wavelets, *Comm. Pure Appl. Math.*, 41, 909-996, 1988.

Davis, T. N., and M. Sugiura, Auroral electrojet activity index AE and its universal time variations, *J. Geophys. Res.*, 71, 785-801, 1966.

Gelpi, C., H. J. Singer, and W. J. Hughes, A comparison of magnetic signatures and DMSP auroral images at substorm onset: Three case studies, *J. Geophys. Res.*, 92, 2447-2460, 1987.

Iyemori, T., and D. R. K. Rao, Decay of the Dst field of geomagnetic disturbance after substorm onset and its implication to storm-substorm relation, *Ann. Geophys.*, 14, 608-618, 1996.

Jacobs, J. A., Y. Kato, S. Matsushita, and V. A. Troitskaya, Classification of geomagnetic micropulstaions, *J. Geophys. Res.*, 69, 180-181, 1964.

Meyer, Y., Orthonormal wavelets, in *Wavelets*, edited by J. M. Combes, A. Grossmann, and Ph. Tchamitchian, pp. 21-37, Springer-Verlag, Berlin, 1989.

Nosé, M., T. Iyemori, M. Takeda, T. Kamei, D. K. Milling, D. Orr, H. J. Singer, E. W. Worthington, and N. Sumitomo, Automated detection of Pi 2 pulsations using wavelet analysis: 1. Method and an application for substorm monitoring, *Earth Planet. Space*, 50, 773-783, 1998.

Osaki, H., K. Yumoto, K. Fukao, K. Shiokawa, F. W. Menk, B. J. Fraser, and the 210° MM magnetic observation group, Characteristics of low-latitude Pi2 pulsations along the 210° magnetic meridian, *J. Geomagn. Geoelectr.*, 48, 1421-1430, 1996.

Saka, O., O. Watanabe, M. Shinohara, H. Tachihara, and D. N. Baker, A comparison of the occurrence of very-low-latitude Pi2 pulsations with magnetic-field and energetic-particle flux variations (30-300 keV) at geosynchronous altitudes, *J. Geomagn. Geoelectr.*, 48, 1431-1441, 1996.

Sakurai, T. and T. Saito, Magnetic pulsation Pi 2 and substorm onset, *Planet. Space Sci.*, 24, 573-575, 1976.

Sasaki, F., T. Maeda, and M. Yamada, Study of time history data using wavelet transform, *J. Struc. Eng. Architec. Inst. Japan*, 38B, 9-20, 1992 (in Japanese with English abstract).

Sato, K. and M. Yamada, Vertical structure of atmospheric gravity waves revealed by the wavelet analysis, *J. Geophys. Res.*, 99, 20,623-20,631, 1994.

Takahashi, K., C. Meng, T. Kamei, T. Kikuchi, and M. Kunitake, Near-real-time auroral electrojet index: An international collaboration makes rapid delivery of auroral electrojet index, *Space Weather*, 2, S11003, doi: 10.1029/2004SW000116, 2004.

Yamada, M. and K. Ohkitani, Orthonormal wavelet analysis of turbulence, *Fluid Dyn. Res.*, 8, 101-115, 1991.

Yamanaka, M. D., T. Shimomai, and S. Fukao, A model of quasi-monochromatic field of middle-atmospheric internal gravity waves, P*roc. of the 1992 STEP Symposium/5th COSPAR Colloquium*, 511-518, 1994.

Yomogida, K., Detection of anomalous seismic phases by the wavelet transform, *Geophys. J. Int.*, 116, 119-130, 1994.

Yumoto, K., K .Takahashi, T. Saito, F. W. Menk, B. J. Fraser, T. A. Potemra, and L. J. Zanetti, Some aspects of the relation between Pi1-2 magnetic pulsations observed at L=1.3-2.1 on the ground and substorm-associated magnetic field variations in the near-Earth magnetotail observed by AMPTE CCE, *J. Geophys. Res.*, 94, 3611-3618, 1989.